Polyhedron 171 (2019) 493–501

Contents lists available at ScienceDirect

Polyhedron

journal homepage: www.elsevier.com/locate/poly

Complexes of palladium(II) chloride with 3-(pyrazol-1-yl)propanamide (PPA) and related ligands

Tyler M. Palombo [a], Phil Liebing [b], Sara J. Hildebrand [a], Quentin R. Patrikus [a], Anders P. Assarsson [a], Ling Wang [b], Donna S. Amenta [a,*], Felix Engelhardt [b], Frank T. Edelmann [b,*], John W. Gilje [a,*]

[a] Department of Chemistry and Biochemistry, James Madison University, MSC 4501, Harrisonburg, VA 22807, United States
[b] Chemisches Institut der Otto-von-Guericke-Universität Magdeburg, Universitätsplatz 2, 39106 Magdeburg, Germany

ARTICLE INFO

Article history:
Received 26 June 2019
Accepted 30 July 2019
Available online 8 August 2019

Keywords:
Pyrazolylpropanamide
Palladium
Crystal structure
Hydrogen bonding
Coordination Modes

ABSTRACT

Four new derivatives of the versatile polyfunctional ligands 3-(pyrazol-1-yl)propanamide (**1**, = PPA) and 3-(3,5-dimethylpyrazol-1-yl)-propanamide (**2**, = Me_2PPA) have been prepared, in which one of the amide hydrogens on **1** and **2** is formally replaced by alkyl residues. X-Ray diffraction studies revealed that, in contrast to **1** and **2**, the *N*-isopropyl substituted derivatives **3** and **4** form supramolecular hydrogen-bonded chains rather than two-dimensional arrays, and the *N*-(2-methyl-4-oxypentan-2-yl) (=MOP) substituted compounds **5** and **6** exist as cyclic dimers in the solid state. Reactions of $PdCl_2$(COD) (COD = 1,5-cyclooctadiene) with 2 equiv. of the corresponding ligands **1–6** in all cases afforded *trans*-$PdCl_2(L)_2$ complexes (**7–12**). X-ray crystal structure determinations of **8**, and **10–12** revealed κ*N*-monodentate coordination of the PPA-type ligands.

1. Introduction

There is a considerable interest in the use of multifunctional ligands containing substituted pyrazole groups because of their potential applications in catalysis [1–7] and their ability to form complexes that mimic structural and catalytic functions in metalloproteins [8–10]. For several years, we have been interested in 3-(pyrazol-1-yl)propanamide (**1**, = PPA), and related ligands (*cf.* Scheme 1, [11–13]). The coordination chemistry of **1** with first transition series metals is diverse. The complexes $CuCl_2(PPA)_2$ and $Co_3Cl_6(PPA)_4$ form in reactions with copper(II) and cobalt(II) chloride, respectively [11]. The reaction of $CuBr_2$ with **1** produced $[CuBr(PPA)_2]Br$ [12], and the perchlorates of iron(II) and cobalt(II) afforded the complexes $[M(PPA)_2(EtOH)_2](ClO_4)_2$ (M = Fe, Co), whereas with nickel(II) chloride, light green $NiCl_2(PPA)_2$ and the dark green cationic nickel(II) complex $[Ni(PPA)_2(H_2O)_4]Cl_2$ were isolated [13]. While complexes of manganese(II) salts with **1** have not been reported, derivatives of **1**, 2-methyl-3-(pyrazol-1-yl)-propanamide and 3-(3,5-dimethylpyrazol-1-yl)-propanamide (**2**, = Me_2PPA), form complexes with this metal ion [14,15]. In a recent study, we reported a series of crystalline $MnCl_2$, $CoCl_2$, $CuCl_2$, and $ZnCl_2$ complexes with ligand **2**, which demonstrated the ability of PPA-type ligands to display different coordination modes [15]. The most characteristic ligand coordination is seven membered ring chelation involving the pyrazolyl nitrogen and the amide oxygen donors (κ*N*,κ*O*-chelating, Scheme 1, a) [11–15]. However, κ*N*:κ*O*-bridging and κ*N*-monodentate modes (Scheme 1, b and c) [15], as well as more complex coordination patterns [11,14] have been observed in a number of compounds. Due to the presence of amide N—H as a potent hydrogen-donating group, the free ligands and complexes participate in highly diverse hydrogen-bonded supramolecular structures in the solid state [11–18]. The chemistry with second and third transition series metals is much less widely investigated. The reaction of $RuCl_2(PPh_3)_3$ with **1** forms $RuCl_2(PPA)(PPh_3)_2$, which also contains a κ*N*,κ*O*-chelating ligand. The crystal structure shows the existence of supramolecular dimers formed by N—H···Cl bonds, but not an extensive hydrogen-bonded network [19]. In contrast, silver(I) forms the dicoordinate complex $[Ag(PPA)_2]NO_3H_2O$, in which the PPA ligand is κ*N*-monodentate, and participates in a complex hydrogen-bonded framework [13].

The present study concentrates on the synthesis and structural characterization of $PdCl_2$ complexes with PPA-derived ligands. In this contribution, we focused on ligands with substituents at differing positions of the molecule. In addition to the frequently used unsubstituted PPA (**1**) and Me_2PPA (**2**), we decided to investigate a series of *N*-substituted derivatives in order to study the influence of the number of hydrogen-bond donors on the resulting molecular and supramolecular structures (Scheme 2). Therefore, we have

* Corresponding authors.
E-mail addresses: amentads@jmu.edu (D.S. Amenta), frank.edelmann@ovgu.de (F.T. Edelmann), giljejw@jmu.edu (J.W. Gilje).

https://doi.org/10.1016/j.poly.2019.07.043
0277-5387/

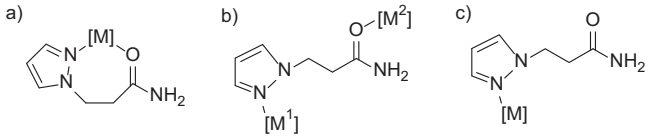

Scheme 1. Schematic representation of different coordination modes observed for 3-(pyrazol-1-yl)propanamide-derived ligands: a) κ*N*,κ*O*-chelating, b) κ*N*:κ*O*-bridging, and c) κ*N*-monodentate.

chosen to use the *N*-isopropyl derivatives of PPA and Me_2PPA (**3**, = PPA^{iPr}, and **4**, = "Me_2PPA^{iPr}"), as well as PPA and Me_2PPA derivatives having an *N*-(2-methyl-4-oxypentan-2-yl) residue (**5**, = "PPA^{MOP}", and **6**, = "Me_2PPA^{MOP}", MOP = 2-methyl-4-oxypentan-2-yl). We were interested in determining if the ligands would chelate as observed with e.g. ruthenium(II) [19] or whether a monodentate mode as seen with silver(I) [13] would occur. In addition, **1** and **2** contain two amide hydrogens and are able to form extended supramolecular structures, which is also to be expected for their $PdCl_2$-complex forms [11–15]. With **3** and **4** there is only a single N—H hydrogen-bond donor, thus, the ability of these ligands to form extensive hydrogen bonding networks should be limited both in their free and complexed states. Finally, **5** and **6** also contain a single amide hydrogen, but have a second carbonyl functional group that provides an additional potential coordination site and hydrogen-bond acceptor moiety.

2. Results and discussion

2.1. Preparation and properties

Ligands. Previously, PPA (**1**) [11–13] and Me_2PPA (**2**) [15] have been reported to form in a straightforward manner by a base-catalyzed Michael addition of acrylamide with pyrazole or 3,5-dimethylpyrazole, respectively (Scheme 3). Similar reactions using *N*-isopropylacrylamide as starting material yielded PPA^{iPr} (**3**) and Me_2PPA^{iPr} (**4**), while the diacetone-derived acrylamide H_2C = CONH-CMe_2-CH_2-COMe led to the formation of PPA^{MOP} (**5**) and Me_2PPA^{MOP} (**6**). Compounds **1–6** have been characterized spectroscopically, by elemental analysis, and X-ray crystallography. The ^1H and ^{13}C NMR and the IR spectra are consistent with the proposed structures.

*Complexes of ligands **1–6** with palladium(II) chloride.* Reactions of $PdCl_2$(COD) (COD = 1,5-cyclooctadiene) with 2 equiv. of the corresponding ligands **1–6** under inert conditions produced yellow products that analyzed for $PdCl_2(L)_2$ (**7–12**; Scheme 4). In the case of $PdCl_2(PPA)_2$ (**7**), the complex is insoluble in common solvents, except for DMSO which appears to displace the ligand. Consequently, this complex has only been characterized by elemental analysis and IR spectroscopy. $PdCl_2(PPA^{iPr})_2$ (**9**) is soluble in several solvents, so NMR spectra have been obtained, but X-Ray quality

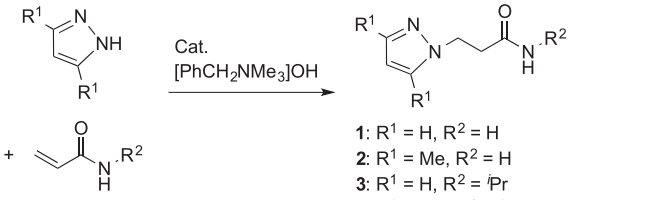

Scheme 3. Preparation of the ligands **1–6**.

crystals have not. $PdCl_2(Me_2PPA)_2$ (**8**), $PdCl_2(Me_2PPA^{iPr})_2$ (**10**), $PdCl_2(PPA^{MOP})_2$ (**11**), and $PdCl_2(Me_2PPA^{MOP})_2$ (**12**) are soluble in several organic solvents and allowed for obtaining NMR spectra and X-ray quality crystals. The ^1H and ^{13}C NMR spectra resemble those of the uncoordinated ligands. The most notable differences involve the chemical shifts of the triplets in the ^1H NMR spectra. These can be assigned to the $-CH_2CH_2-$ groups that connect the pyrazolyl ring to the amide functionality. The most downfield triplet, which we assign to the CH_2 group attached to the pyrazolyl nitrogen, shifts downfield by nearly 0.7 ppm, while the upfield triplet, which we assign to the CH_2 group attached to the amide carbon, exhibits a downfield shift of nearly 1 ppm. While the spectra are consistent with complex formation, they do not provide substantive information on structural details of the molecules. The IR spectra of the free ligands and the palladium complexes show typical bands for the amide functionality. Comparison of the free ligand **3** and complex **9** revealed a significant increase to higher wavenumbers in the N—H stretching vibrations (3321 cm^{-1} and 3375 cm^{-1}, respectively). A similar behavior was observed for the complexes **10–12**. This N—H absorption shift is consistent with the formation of the N—H hydrogen bridge to the central metal Pd. The IR spectra also show bands at 1638 cm^{-1} and 1543 cm^{-1} in **3** and 1635 cm^{-1} and 1564 cm^{-1}in **9**, which could be assigned to the C=O stretching vibration (amide I) and the interaction between $\nu_{C\text{-}N}$ and δ_{CNH} (amide II), respectively [20].

2.2. Crystal structures

The crystal structures of PPA (**1**) [13] and Me_2PPA (**2**) [21] have been published previously, and those of the *N*-substituted derivatives **3–6** are reported here (Figs. 1–4, see Table 1 for experimental details). Regarding the orientation of the *N*-alkyl substituent relative to the amide oxygen, all four compounds exist as the *s-cis* rotamer in the crystal. While the bond distances and angles are unremarkable and very similar between the molecules, the hydrogen bonding patterns in the crystal structures differ between the various derivatives. In compounds **1** and **2**, the molecules are linked into two-dimensional supramolecular arrays by N—H···O

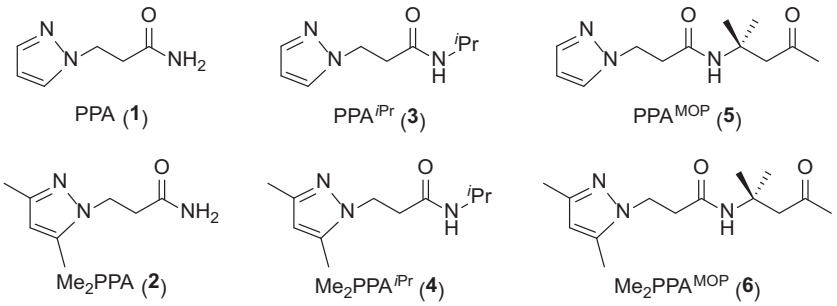

Scheme 2. Schematic representation of the ligands **1–6** used in this study.

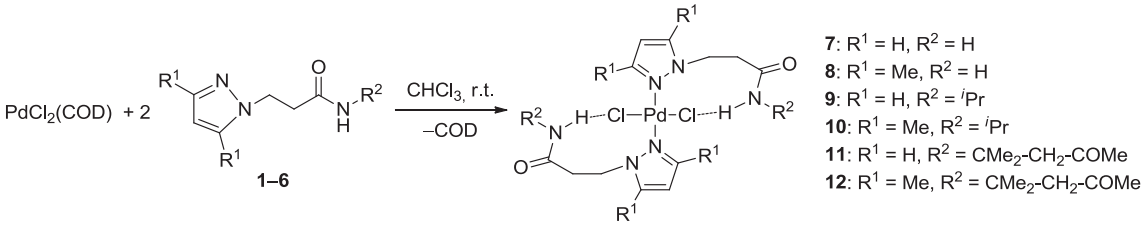

Scheme 4. Preparation of the palladium(II) complexes **7–12**.

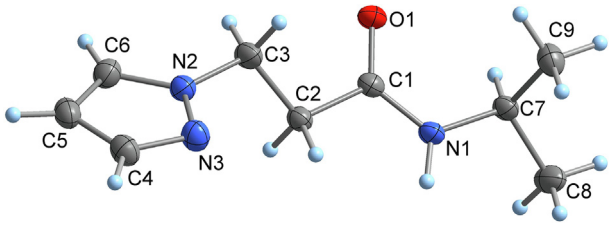

Fig. 1. Molecular structure of PPA^{iPr} (**3**) in the crystal, showing the atom-numbering scheme. Displacement ellipsoids with 50% probability. Selected interatomic distances (pm): C1–O1 123.6(1), C1–N1 133.8(2), N2–N3 135.3(2), N3–C4 133.2(2).

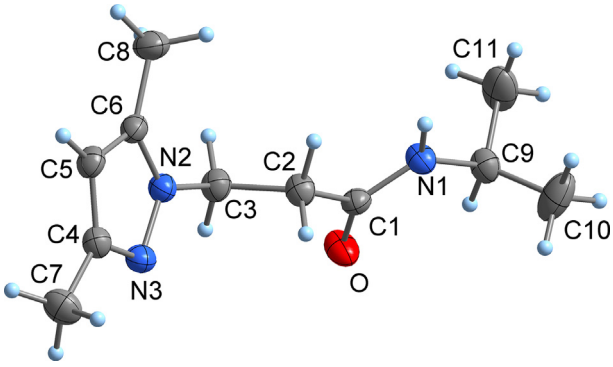

Fig. 2. Molecular structure of Me_2PPA^{iPr} (**4**) in the crystal, showing the atom-numbering scheme. Displacement ellipsoids with 50% probability. Selected interatomic distances (pm): C1–O 122.7(2), C1–N1 132.9(2), N2–N3 136.0(2), N3–C4 133.4(2).

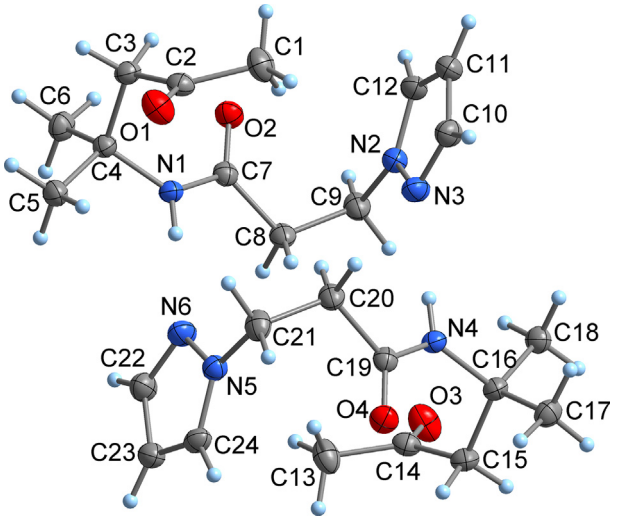

Fig. 3. Molecular structure of PPA^{MOP} (**5**) in the crystal, showing two molecules in the asymmetric unit together with the atom-numbering scheme. Displacement ellipsoids with 50% probability. Selected interatomic distances (pm): Molecule 1: O1–C2 121.5(2), O2–C7 122.1(2), N1–C7 134.8(2), N2–N3 135.1(2), N3–133.2(2); Molecule 2: O3–C14 121.5(2), O4–C19 122.0(2), N4–C19 134.6(2), N5–N6 134.7(2), N5–C24 133.8(2).

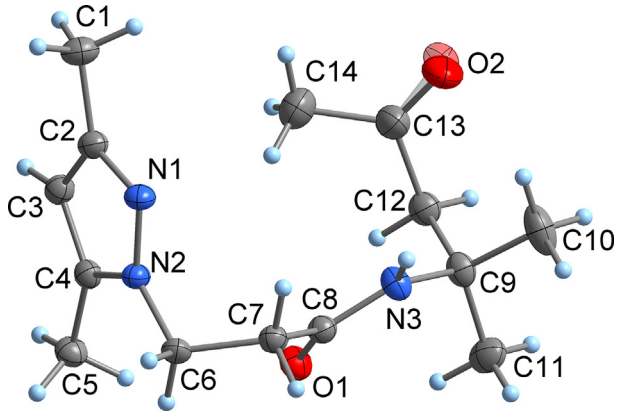

Fig. 4. Molecular structure of Me_2PPA^{MOP} (**5**) in the crystal, showing disorder of the keto group over two orientations together with the atom-numbering scheme. Displacement ellipsoids with 50% probability. Selected interatomic distances (pm): O1–C8 122.7(2), O2–C13 124.2(5), O2′–C13 121.3(5), N1–N2 136.1(2), N2–C4 135.4 (2), N3–C8134.2(2).

and N—H···N bonds [13,21]. As anticipated, this is not the case for **3–6**, since one of the two hydrogen bond donors is formally replaced by an alkyl group. Therefore, in PPA^{iPr} (**3**), the molecules are stacked together to a linear chain by N—H···O bonds between the amide groups, while the crystal structure of Me_2PPA^{iPr} (**4**) displays helical chains formed by N—H···N bonds between amide carbonyl and pyrazolyl moieties (Fig. 5). In contrast, PPA^{MOP} (**5**) and Me_2PPA^{MOP} (**6**) both exist as cyclic supramolecular dimers in the crystal. These are formed by N—H···N bonds, while the amide and keto oxygens do not contribute to hydrogen bonding (Fig. 6). The hydrogen-bonded N···O distance in **3** is 296.0(1) pm and therefore comparable with the values observed in **1** (293.4(1) pm) [13] and **2** (293.6(3) pm) [21]. The N···N separations in **4–6** are in a narrow range of 297.7(2)–300.3(2) pm and resemble that observed in **1** (299.3(1) pm) [13], while the value observed in **2** (308.4(3) pm) is significantly larger [21].

Crystal structure determinations of the palladium(II) complexes **8** and **10–12** revealed that all these compounds exist as well-defined mononuclear, centrosymmetric complexes of the composition $PdCl_2(L)_2$ (Figs. 7–9, for experimental details see Table 1). While the crystal quality of $PdCl_2(Me_2PPA^{MOP})_2$ (**12**) was not adequate for full structure refinement, the data obtained for $PdCl_2(Me_2PPA)_2$ (**8**), $PdCl_2(Me_2PPA^{iPr})_2$ (**10**), and $PdCl_2(PPA^{MOP})_2$ (**11**) allowed for a detailed analysis of the bonding parameters and hydrogen-bond geometries. In all four complexes, the two PPA-derived ligands are attached to the palladium center in a κ*N*-monodentate mode, which has been previously observed for the copper (II) complex $CuCl_2(Me_2PPA)_2{\cdot}2H_2O$ [15]. Just like in the reference compound, a square-planar coordination of the metal center is completed by two chloro ligands, whereas the two coordinated pyrazolyl groups are in a *trans* arrangement (configuration index SP-4–12). The Pd-N bond lengths in **8**, **10**, and **11** are virtually equal at 200.2(2)–200.9(1) pm, thus being not significantly

Table 1
Crystallographic details for the compounds reported in this work.

Compound	**3**	**4**	**5**	**6**	**8**	**10**	**11**
CCDC deposition number	1,912,534	1,912,535	1,912,536	1,912,537	1,912,538	1,912,539	1,912,540
Molecular formula sum	$C_9H_{15}N_3O$	$C_{11}H_{19}N_3O$	$C_{12}H_{19}N_3O_2$	$C_{14}H_{23}N_3O_2$	$C_{16}H_{26}Cl_2N_6O_2Pd$	$C_{22}H_{38}Cl_2N_6O_2Pd$	$C_{24}H_{38}Cl_2N_6O_4Pd$
Formula weight/g mol^{-1}	181.24	209.29	237.30	265.35	511.73	595.88	651.90
Crystal system	monoclinic	monoclinic	triclinic	monoclinic	monoclinic	triclinic	triclinic
Space group	$P2_1/c$	$P2_1/n$	$P\bar{1}$	$P2_1/n$	$P2_1/c$	$P\bar{1}$	$P\bar{1}$
Cell parameters a/Å	4.9352(2)	10.062(2)	8.718(4)	8.230(3)	11.2723(5)	7.2409(4)	8.168(4)
b/Å	17.338(1)	11.339(2)	10.409(6)	17.882(4)	6.5591(2)	8.4791(4)	8.969(4)
c/Å	11.4111(5)	11.308(2)	14.203(7)	10.503(3)	14.5479(7)	11.5221(6)	10.382(5)
α/deg.	90	90	83.79(5)	90	90	93.677(4)	76.22(4)
β/deg.	99.505(3)	113.00(3)	84.29(4)	109.29(3)	100.723(4)	94.373(4)	83.26(4)
γ/deg.	90	90	77.21(4)	90	90	107.371(4)	81.16(3)
Cell volume/Å^3	963.02(8)	1187.6(5)	1246(1)	1459.0(8)	1056.83(8)	670.37(6)	727.3(6)
Molecules per cell z	4	4	4	4	2	1	1
Electrons per cell F_{000}	392	456	512	576	520	308	336
Calcd. density ρ/g cm^{-3}	1.250	1.171	1.265	1.208	1.608	1.476	1.488
μ/mm^{-1} (Mo-K$_\alpha$)	0.085	0.077	0.088	0.082	1.154	0.921	0.861
Crystal color and shape	colorless rod	colorless prism	colorless block	colorless block	yellow plate	yellow rod	yellow block
Crystal size/mm	0.37 × 0.26 × 0.16	0.54 × 0.48 × 0.33	0.19 × 0.17 × 0.13	0.20 × 0.16 × 0.15	0.39 × 0.24 × 0.06	0.20 × 0.11 × 0.11	0.21 × 0.18 × 0.17
Temperature/K	133(2)	173(2)	100(2)	100(2)	133(2)	153(2)	100(2)
θ range/deg.	3.621 … 29.230	2.302 … 25.997	2.014 … 29.285	2.278 … 29.233	3.610 … 26.998	2.956 … 27.999	2.358 … 29.148
Reflections collected	6977	5884	10,941	15,321	7870	8066	7565
Reflections unique	2575	2295	6574	3916	2297	3244	3790
Reflections with $I > 2\sigma(I)$	2031	1791	5875	3665	2124	3081	3749
Completeness of dataset	99.2%	98.4%	96.6%	98.7%	99.5%	99.8%	96.8%
R_{int}	0.0364	0.0343	0.0290	0.0471	0.0439	0.0383	0.0337
Parameters; Restraints	121; 0	141; 0	314; 444	187; 274	126; 0	155; 0	172; 232
R_1 (all data, $I > 2\sigma(I)$)	0.0641; 0.0440	0.0597; 0.0426	0.0627; 0.0549	0.0669; 0.0621	0.0275; 0.0251	0.0240; 0.0220	0.0270; 0.0266
wR_2 (all data, $I > 2\sigma(I)$)	0.1030; 0.0932	0.1087; 0.1017	0.1280; 0.1240	0.1311; 0.1291	0.0677; 0.0664	0.0581; 0.0575	0.0687; 0.0685
GooF (F^2)	1.053	1.039	1.156	1.258	1.065	1.047	1.072
Max. residual peaks	−0.195; 0.225	−0.203; 0.203	−0.229; 0.323	−0.226; 0.293	−0.929; 0.610	−0.949; 0.546	−1.161; 0.494
Extinction coefficient	0.023(4)	0.026(6)	–	–	–	–	–

dependent on the substituent pattern of the PPA ligand. The same is true for the Pd-Cl bonds, which were observed at 229.6(1)–230.1 (1) pm. Consequently, the coordination environment around the Pd center is similar to that in the related complex *trans*-$PdCl_2$(pyrazole)$_2$ (Pd-Cl 230.79(6) pm, Pd-N 202.8(2) pm) [22]. However, the molecular structures of **8**, **10**, and **11** are supported by intramolecular N—H···Cl bonding. The significance of this secondary bonding interaction is corroborated by the pyrazole ring being rotated out of the palladium's coordination plane by about 70°, while the $PdCl_2N_2$ and C_3N_2 planes are almost coplanar in *trans*-$PdCl_2$(pyrazole)$_2$ (angle between planes 9.1(1)°) [22]. The intramolecular N···Cl distances are 347.6(2) pm (**8**), 335.9(2) pm (**10**), and 339.7(2) pm (**11**), respectively, and therefore larger than in the related copper(II) complex (N···Cl 331.8(2) pm) [15]. As a consequence of the "twisted" arrangement of the pyrazolyl rings, the palladium center is efficiently shielded by the ethylene backbones, and for complexes **8** and **10** additionally by the substituents in 5-position of the pyrazolyl groups. This effect is potentially important for reactions in which the fifth and sixth coordination site at palladium are involved. Accordingly, the crystal structures of **8**, **10**, and **11** do not display any secondary Pd···Cl, Pd···O, or Pd···N bonds.

While the structures of the *N*-substituted derivatives **10** and **11** do not allow for further aggregation of the molecules through hydrogen bonding, the molecules of complex **8** are linked into a supramolecular layer structure by N—H···O bonds between the $CONH_2$ groups (Fig. 10). The N···O separations are 287.0(4) pm and therefore slightly closer than in the free Me_2PPA ligand (N···O 293.6(3) pm) [21]. The bonding interactions between the layers are rather weak, being limited to unspecific van-der-Waals interactions with the pyrazolyl-methyl groups facing each other (Fig. 11). It is to be expected that $PdCl_2$(PPA)$_2$ (**7**) also shows extensive aggregation through hydrogen bonding, which is a reasonable explanation for the low solubility of this complex.

3. Conclusions

As a continuation of our studies of the coordination chemistry of 3-(pyrazol-1-yl)propanamide (PPA) and related compounds, we have prepared ligands in which one of the amide hydrogens on PPA (**1**) and Me_2PPA (**2**) is formally replaced by alkyl residues. These substitutions drastically reduce the ability of the compounds to form complex extended H-bond networks. Thus, in contrast to **1** and **2**, the *N*-isopropyl substituted derivatives **3** and **4** form supramolecular hydrogen-bonded chains rather than two-dimensional arrays, and the *N*-(2-methyl-4-oxypentan-2-yl) (=MOP) substituted compounds **5** and **6** exist as cyclic dimers in the solid state. All of the ligands **1–6** form *trans*-$PdCl_2(L)_2$ complexes (**7–12**). X-ray crystal structure determinations of **8**, and **10–12** revealed a κ*N*-monodentate coordination of the PPA-type ligands in each case, and the same is to be expected for **7** and **9**. Consequently, the coordination chemistry of PPA and related ligands with palladium(II) is less diverse and more predictable than with first-row transition metals, which allows for controlled and targeted bottom-up construction of supramolecular hydrogen-bonded structures.

4. Experimental section

4.1. General methods and materials

4.1.1. Physical methods

Microanalyses were performed by Galbraith Laboratories, Inc., Knoxville, TN, USA. IR spectra were recorded on a Bruker Alpha FT-IR using an ATR accessory between 4000 cm^{-1} and 400 cm^{-1} at 2 cm^{-1} resolution. NMR spectra were recorded on Bruker Advance 300 and 400 NMR spectrometers and analyzed using SpinWorks 4.0.3.0. Single-crystal X-ray intensity data were collected on a STOE IPDS 2 T diffractometer equipped with a 34 cm

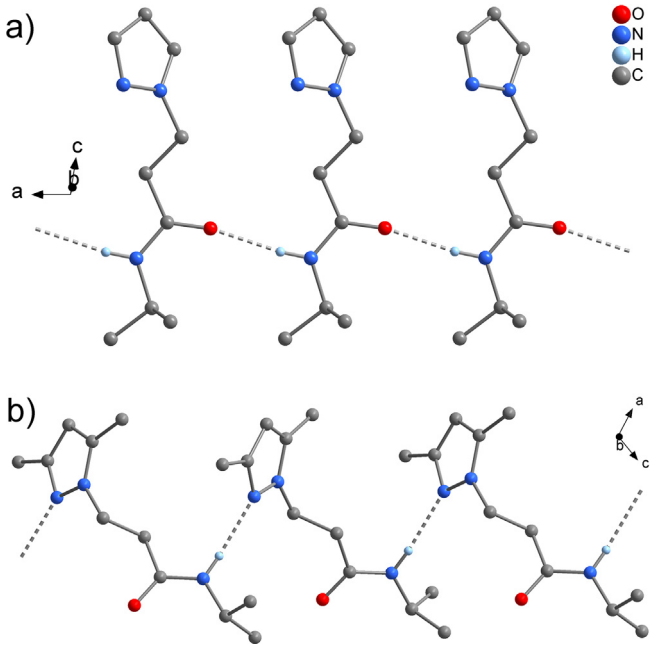

Fig. 5. Representation of the supramolecular chain structures of a) PPA^{iPr} (**3**) and b) Me_2PPA^{iPr} (**4**) in the crystal (H atoms attached to C atoms omitted for clarity).

image plate detector, using graphite-monochromated Mo-K_α radiation (λ = 0.71073 Å). Numerical absorption correction was applied for the palladium complexes **8**, and **10–12** [23]. The structures were solved with SIR-97 [24] or SHELXT-2018 [25] and refined by full matrix least-squares methods on F^2 using SHELXL-2018 [26].

4.1.2. Materials

Dichloro(1,5-cyclooctadiene)palladium(II) was used as received from Strem Chemicals. Acrylamide, *N*-isopropylacrylamide, diacetone acrylamide, bis(benzonitrile)dichloropalladium(II), and trimethylbenzylammonium hydroxide (40% in methanol, Triton B) were used as received from Sigma Aldrich. Chloroform (99.8%) was used as received from Acros Organics. 3,5-Dimethylpyrazole was used as received from Fluka Analytical. PPA (**1**) [10] and Me_2-PPA (**2**) [21] were prepared as described in the literature.

4.1.3. Synthesis of PPA^{iPr} (3)

Pyrazole (3.10 g, 46 mmol), *N*-isopropylacrylamide (5.19 g, 46 mmol), and trimethylbenzylammonium hydroxide (1 mL, 40%

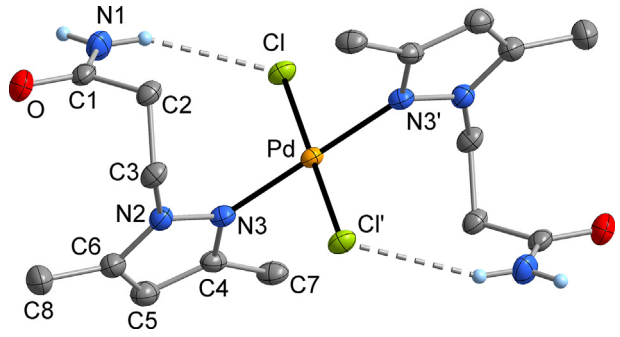

Fig. 7. Molecular structure of $PdCl_2(Me_2PPA)_2$ (**8**) in the crystal, showing the atom numbering scheme. Displacement ellipsoids with 50% probability, H atoms attached to C atoms omitted for clarity. Symmetry operator: '2–x, –y, –z. The Pd atom is located on a crystallographic center of inversion at (0, 0, 0). Selected interatomic distances (pm) and angles (deg.): Pd–Cl 229.76(4), Pd–N3 200.8(2), Cl–Pd–Cl 180.00, Cl–Pd–N3 90.36(5), Cl–Pd–N' 89.64(5), N3–Pd–N3′ 180.00, O–C1 122.8(2), N1–C1 133.2(3), N2–N3 135.6(2), N3–C4 133.1(2), N1···Cl 347.6(2).

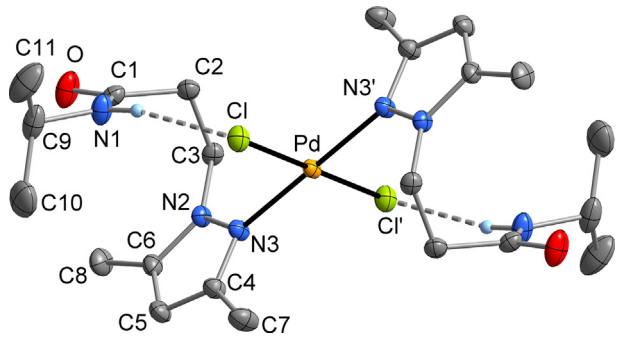

Fig. 8. Molecular structure of $PdCl_2(Me_2PPA^{iPr})_2$ (**10**) in the crystal, showing the atom numbering scheme. Displacement ellipsoids with 50% probability, H atoms attached to C atoms omitted for clarity. The Pd atom is located on a crystallographic center of inversion at (0, 0, 0.5). Symmetry operator: ' –x, 2–y, 1–z. Selected interatomic distances (pm) and angles (deg.): Pd–Cl 230.31(4), Pd–N3 200.9(1), Cl–Pd–Cl' 180.00, Cl–Pd–N3 90.43(4), Cl–Pd–N3′ 89.57(4), N3–Pd–N3′ 180.00, O–C1 122.7(2), N1–C1 133.7(2), N2–N3 136.1(2), N3–C4 133.3(2), N1···Cl 335.9(2).

in methanol, "Triton B") were heated to reflux for 3 h. The resulting yellow oil was dissolved in diethyl ether and cooled to –10 °C until the product solidified. The crude product was vacuum filtered, washed with cold diethyl ether, and dried *in vacuo* (5.05 g, 61%). Crystals suitable for X-ray diffraction were obtained by recrystallization from diethyl ether. Elem. Anal. Calcd. for $C_9H_{15}N_3O$ (M = 181.24 g mol^{-1}): C, 59.64; H, 8.34; N, 23.19. Found: C, 59.00; H, 8.38; N, 22.69%. M.p. = 62 °C. **IR** (cm^{-1}): ν = 3321 vs

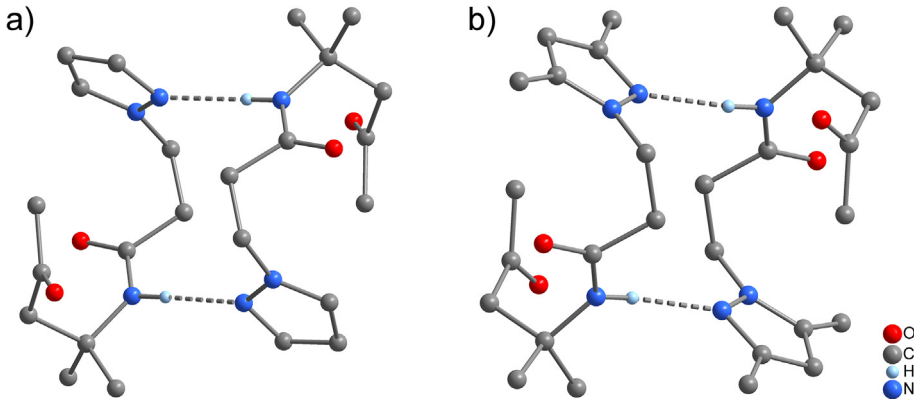

Fig. 6. Representation of the supramolecular dimer structures of a) PPA^{MOP} (**5**) and b) Me_2PPA^{MOP} (**6**) in the crystal (H atoms attached to C atoms omitted for clarity).

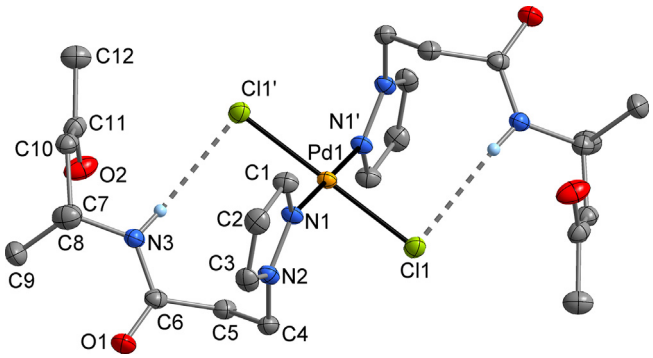

Fig. 9. Molecular structure of $PdCl_2(PPA^{MOP})_2$ (**11**) in the crystal, showing the atom numbering scheme. Displacement ellipsoids with 50% probability, H atoms attached to C atoms omitted for clarity. The Pd atom is located on a crystallographic center of inversion at (0.5, 0.5, 0.5). Symmetry operator: ' 1–x, 1–y, 1–z. Selected interatomic distances (pm) and angles (deg.): Pd1–Cl1 229.6(1), Pd1–N1 200–2(2), Cl1–Pd1–Cl1′ 180.00, Cl1–Pd1–N1 90.89(6), Cl1–Pd–N1′ 89.11(6), N1–Pd1–N1′ 180.00, O1–C6 122.9(2), O2–C11 120.9(2), N1–N2 135.1(2), N1–C1 133.1(2), N3–C6 133.8(2), N1···Cl 339.7(2).

(ν_{N-H}), 3134 w, 3118 w, 3075 w, 2975 vs, 2943 w, 2879 w, 1771 w, 1638 vs ($\nu_{C=O}$), 1543 vs ($\nu_{C-N} + \delta_{CNH}$), 1510 m. 1474 w, 1451 m, 1425 w, 1401 m, 1386 s, 1366 m, 1339 w, 1282 s, 1237 s, 1215 m, 1173 m, 1133 s, 1055 s, 1030 s, 970 m, 945 w, 911 m, 925 w, 911 m, 844 w, 763 vs, 684 s, 656 vs, 611 s, 488 m, 448 m, 414 s. **^{1}H NMR** (400 MHz, $CDCl_3$): δ = 1.09 (6H, d, J = 6.58 Hz, $CH(CH_3)_2$), 2.72 (2H, t, J = 6.3 Hz, α-CH_2), 3.99 (1H, m, J = 6.58 Hz, $CH(CH_3)_2$), 4.46 (2H, t, J = 6.3 Hz, β-CH_2), 6.23 (1H, dd, J = 2.29 Hz, J = 1.90 Hz, 4-C*H*), 7.43 (1H, dd, J = 2.29 Hz, J = 0.60 Hz, C*H*), 7.53 (1H, dd, J = 1.90 Hz, J = 0.60 Hz, C*H*) ppm. **^{13}C NMR** (100 MHz, $CDCl_3$): δ = 22.5 (s, $CH(CH_3)_2$, 37.6 (s, α-CH_2), 41.4 (s, β-CH_2) , 48.2 (s, *C*H $(CH_3)_2$, 105.3 (s, 4-*C*H), 130.3 (s, *C*H), 139.7 (s, *C*H), 169.1 (s, *C*=O) ppm.

4.1.4. Synthesis of Me_2PPA^{iPr} (4)

A mixture of *N*-isopropylacrylamide (2.86 g, 25 mmol), 3,5-dimethylpyrazole (2.40 g, 25 mmol), and trimethylbenzylammonium hydroxide (1 mL, 40% in methanol, "Triton B") was submerged in a boiling water bath for 5 h. The reaction mixture solidified on cooling. The residue was washed with diethyl ether, and dried in vacuo to give 4.41 g (84%) of **4**. Recrystallization from

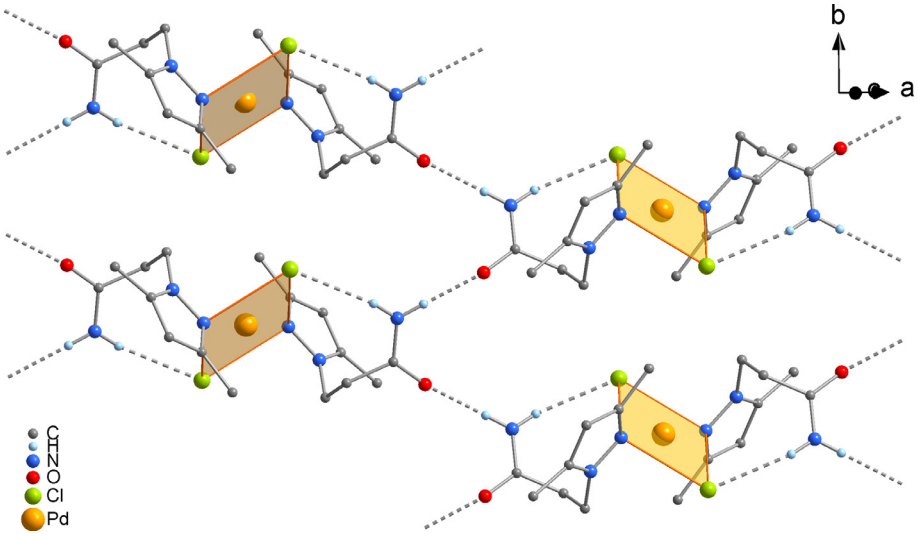

Fig. 10. Representation of the intermolecular N—H···O hydrogen bonds of $PdCl_2(Me_2PPA)_2$ (**8**) viewed in a projection on (1 0 –2) (H atoms attached to C atoms omitted for clarity). The 2D supramolecular structure extends parallel to (1 0 –2).

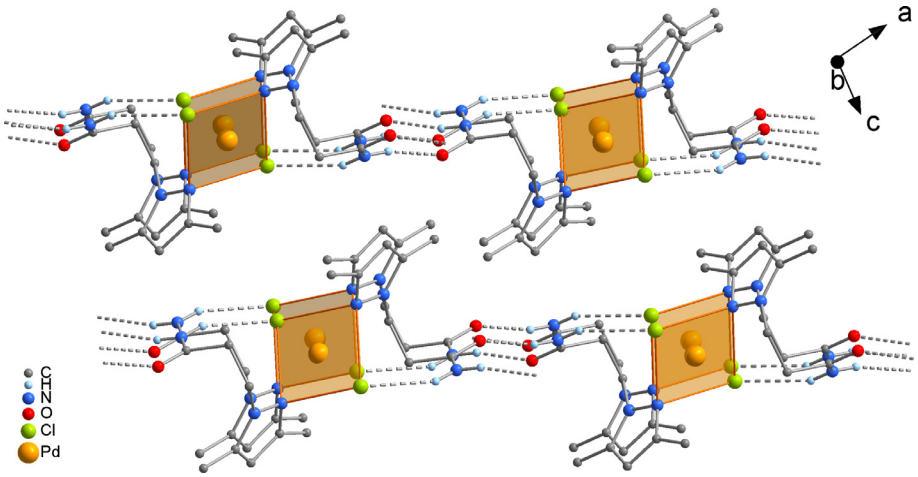

Fig. 11. Illustration of two proximate layers of **8** shown in Fig. 10, viewed in a projection on (0 1 0), i.e. along the planes (H atoms attached to C atoms omitted for clarity).

methylene chloride/diethyl ether (2:1) solution yielded colorless crystals suitable for X-ray diffraction analysis. Elem. Anal. Calcd. for $C_{11}H_{19}N_3O$ (M = 209.29 g mol^{-1}): C, 63.13; H, 9.15; N, 20.08. Found: C, 63.18; H, 8.9; N, 20.09%. M.p. 123–125 °C. **IR** (ATR, cm^{-1}): ν = 3232 m (ν_{N-H}), 3203 m, 3117 m, 3054 m, 2982 m, 2969 m, 2930 m, 2874 w, ν 1658 vs ($\nu_{C=O}$), 1549 s (ν_{C-N} + δ_{CNH}), 1490 w, 1458 s, 1430 m, 1419 m, 1380 vs, 1367 s, 1330 m, 1257 w, 1340 vs, 1204 vw, 1163 m, 1132 m, 1121 m, 1055 w, 1036 w, 1016 s, 989 m, 926 w, 852 w, 818 s, 771 m, 652 s, 608 s, 588 w, 488 w, 474 m, 440 s. **^{1}H NMR** (400 MHz, $CDCl_3$): δ = 1.05 (6H, d, J = 6.58 Hz, CH(CH_3)$_2$), 2.22 (3H, s, 5-CH_3), 2.24 (3H, s, 3-CH_3), 2.69 (2H, t, J = 6.45 Hz, α-CH_2), 3.93 (1H, sept, J = 6.58 Hz, CH(CH$_3$)$_2$), 4.23 (2H, t, J = 6.44 Hz, β-CH_2), 5.78 (1H, s, 4-CH), 5.82 (1H, br, s, NH) ppm. **^{13}C NMR** (100 MHz, $CDCl_3$): δ = 10.9 (s, 5-CH_3), 13.4 (s, 3-CH_3), 22.5 (s, CH(CH_3)$_2$), 37.4 (s, α-CH_2), 41.4 (s, β-CH_2), 44.4 (s, CH(CH$_3$)$_2$), 104.9 (s, 4-CH), 139.8 (s, 5-C-CH$_3$), 147.8 (s, 3-C-CH$_3$), 169.5 (s, C=O) ppm.

4.1.5. Synthesis of PPA^{MOP} (5)

A mixture of pyrazole (1.36 g, 20 mmol), diacetone acrylamide (3.39 g, 20 mmol), and trimethylbenzylammonium hydroxide (1.2 mL, 40% in methanol, "Triton B") was heated for 3 h in a water bath maintained at 44–47 °C. A white solid formed after cooling to room temperature, which was washed three times with diethyl ether. After three recrystallizations from diethyl ether/hexanes, 2.94 g (62%) of **5** was obtained. Single crystals suitable for X-ray diffraction were obtained following these recrystallizations. Elem. Anal. Calcd. for $C_{12}H_{19}N_3O_2$ (M = 237.30 g mol^{-1}): C, 60.74; H, 8.07; N, 17.71; Found: C, 60.97; H, 8.21; N, 17.72%. M.p. 74–76 °C. **IR** (ATR, cm^{-1}): ν = 3256 m (ν_{N-H}), 3214 m, 3132 w, 3051 m, 2979 m, 2941 m, 1697 vs ($\nu_{C=O}$, MOT), 1675 vs ($\nu_{C=O}$), 1543 s (ν_{C-N} + δ_{CNH}), 1515 m, 1467 m, 1439 m 1410 m, 1401 m, 1384 m, 1372 m, 1360 m, 1319 m, 1281 m, 1252 m, 1206 m, 1183 m, 1153 m, 1130 m, 977 m, 950 m, 935 m, 918 m, 895 m, 841 m, 772 vs, 753 vs, 670 m, 651 m, 616 m, 563 m, 537 m, 498 w, 484 w, 479 w, 476 w, 466 w, 462 w, 456 w. **^{1}H NMR** (400 MHz, Acetone-d$_6$): δ = 1.32 (6H, s, C(CH_3)$_2$), 2.02 (3H, s, CH_3 (MOP)), 2.65 (2H, t, J = 6.73 Hz, α-CH_2), 2.96 (2H, s, CH_2 (MOP)), 4.36 (2H, t, J = 6.73 Hz, β-CH_2), 6.17 (1H, dd, J = 1.8 Hz, J = 2.2 Hz, 4-CH), 6.89 (1H, br, s, NH), 7.39 (1H, dd, J = 0.6 Hz, J = 1.8 Hz, 3-CH), 7.57 (1H, dd, J = 2.2 Hz, J = 0.6 Hz, 5-CH) ppm. **^{13}C NMR** (100 MHz, Acetone-d$_6$): δ = 26.6 (s, C(CH$_3$)$_2$), 30.7(s, CH$_3$ (MOP)), 37.0 (s, α-CH$_2$), 47.7 (s, β-CH$_2$), 50.4 (s, CH$_2$(MOP)), 51.6 (s, C(CH$_3$)$_2$), 104.5 (s, 4-CH), 129.4 (s, 3-CH), 138.5 (s, 5-CH), 169.3 (s, C=O), 206.3 (s, C=O (MOP)) ppm.

4.1.6. Synthesis of Me$_2$PPA^{MOP} (6)

A mixture of 3,5-dimethylpyrazole (2.85 g, 33 mmol), diacetone acrylamide (5.04 g, 33 mmol), and trimethylbenzylammonium hydroxide (1 mL, 40% in methanol, "Triton B") was heated to reflux for 2.5 h. The reaction mixture was cooled to room temperature producing a waxy solid. The solid was triturated with two 10 mL aliquots of diethyl ether yielding **6** as a white solid (4.67 g, 59%). Single crystals appropriate for X-Ray diffraction were obtained by recrystallization from diethyl ether. Elem. Anal. Calcd. for $C_{14}H_{23}N_3O_2$ (M = 265.36 g mol^{-1}): C, 63.37; H, 8.74; N, 15.84. Found: C, 63.08, H, 8.57, N, 15.43%. M.p. 99–100 °C. **IR** (ATR, cm^{-1}): ν = 3246 w (ν_{N-H}), 3048 w, 2999 w, 2966 w, 2935 w, 1702 s ($\nu_{C=O}$, MOP) , 1672 vs ($\nu_{C=O}$), 1552 vs (ν_{C-N} + δ_{CNH}), 1468 m, 1440 m, 1429 m, 1412 m, 1380 s, 1361 s, 1354 s, 1299 m, 1251 s, 1207 m, 1175 w, 1150 w, 1129 w, 1054 w, 1032 w, 992 w, 944 w, 893 w, 839 w, 791 s, 732 w, 706 w, 673 w, 653 w, 630 w, 613 w, 600 w, 569 m, 538 m, 529 w, 510 w, 504 w. **^{1}H NMR** (400 MHz, $CDCl_3$): δ = 1.30 (6H, s, C(CH_3)$_2$), 2.05 (3H, s, CH_3 (MOP)); 2.20 (3H, s, 5-CH_3), 2.23 (3H, s, 3-CH_3), 2.66 (2H, t, J = 6.62 Hz, α-CH_2), 2.89 (2H, s, CH_2 (MOP)), 4.19 (2H, t, J = 6.62 Hz, β-CH_2), 5.75 (1H, s, 4-CH) ppm. **^{13}C NMR** (100 MHz, $CDCl_3$): δ = 10.9 (s, 5-CH$_3$), 13.4 (s, 3-CH$_3$), 27.1 (s, C(CH$_3$)$_2$), 31.6 (s, CH$_3$ (MOP)), 37.8 (s, α-CH$_2$), 37.9 (s, CH$_2$(MOP)), 44.3 (s, β – CH$_2$), 52.1 (s, C(CH$_3$)$_2$), 104.8 (s, 4-CH), 139.5 (s, 5-C-CH$_3$), 147.8 (s, 3-C-CH$_3$), 170.1 (s, C=O), 207.6 (s, C=O (MOP)) ppm.

4.1.7. Synthesis of PdCl$_2$(PPA)$_2$ (7)

PPA (**1**; 56 mg, 0.40 mmol) and dichloro(1,5-cyclooctadiene)-palladium(II) (75 mg, 0.26 mmol) were dissolved in 25 mL of chloroform and stirred under nitrogen for 3 d. The solution was concentrated and a yellow precipitate of **7** formed to yield 71 mg (78%). This complex is insoluble in common solvents. While it does dissolve in DMSO, this solvent apparently displaces the ligand and satisfactory NMR spectra could not be obtained. Elemental Anal. Calcd for $C_{12}H_{18}Cl_2N_6O_2Pd$ (M = 455.64 g mol^{-1}): C, 31.63; H, 3.98; N, 18.44. Found: C, 31.64; H, 3.91; N, 17.93%. M.p. 133–135 °C. **IR** (ATR, cm^{-1}): ν = 3371 m (ν_{N-H}), 3340 m, 3190 m, 3120 w, 2918 w, 2360 m, 2342 w, 1658 vs ($\nu_{C=O}$), 1616 m (ν_{C-N} + δ_{CNH}), 1520 m, 1430 w, 1415 s, 1372 m, 1302 m, 1270 m, 1217 m, 1191 w, 1173 w, 1116 w, 1088 m, 1041 w, 1013 w, 938 w, 901 w, 864 w, 794 w, 777 w, 760 s, 668 w, 654 w, 604 w, 535 m, 473 m.

4.1.8. Synthesis of PdCl$_2$(Me$_2$PPA)$_2$ (8)

Me$_2$PPA (**2**; 86 mg, 0.50 mmol) and dichloro(1,5-cyclooctadiene)palladium(II) (73 mg, 0.26 mmol) were dissolved in 20 mL of chloroform and stirred under nitrogen for 3 d. Evaporation of the solvent yielded 89 mg (75%) of an orange solid. Yellow needle-like crystals suitable for X-Ray diffraction were obtained from a methanol solution by slow evaporation. Elemental Anal. Calcd. for $C_{16}H_{26}Cl_2N_6O_2Pd$ (M = 511.75 g mol^{-1}): C, 37.55; H, 5.12; N, 16.42. Found: C, 37.50; H, 5.21; N, 16.0%. M.p. 261.2–263.5 °C. **IR** (ATR, cm^{-1}): ν = 3384 m (ν_{N-H}), 3166 m, 2962 m, 1704 m, 1687 w ($\nu_{C=O}$), 1554 w, 1470 w, 1414 m, 1395 m, 1351 w, 1316 w, 1258 s, 1206 w, 1086 w, 1013 s, 864 w, 792 s, 702 w, 660 w, 602 m, 532 w, 476 m. **^{1}H NMR** (400 MHz, $CDCl_3$): δ = 2.35 (3H, s, 5-CH_3), 2.83 (3H, s, 3-CH_3), 3.79 (2H, t, J = 6.38 Hz, α-CH_2), 4.98 (2H, t, J = 6.38 Hz, β-CH_2), 5.14 (1H, s, br, NH), 5.91 (1H, s, 4-CH), 6.38 (1H, s, br, NH) ppm. **^{13}C NMR** (100 MHz, $CDCl_3$): 11.8 (s, 5-CH$_3$), 15.1 (s, 3-CH$_3$), 36.1 (s, α-CH$_2$), 45.3 (s, β-CH$_2$), 107.6 (s, 4-CH), 145.1 (s, 5-C-CH$_3$), 150.4 (s, 3-C-CH$_3$), 172.0(s, C=O) ppm.

4.1.9. Synthesis of PdCl$_2$(PPA^{iPr})$_2$ (9)

PPA^{iPr} (**3**; 91 mg, 0.50 mmol) and dichloro(1,5-cyclooctadiene)-palladium(II) (75 mg, 0.26 mmol) were dissolved in 20 mL of chloroform and stirred under nitrogen for three days. Evaporation of the solvent yielded 92 mg (68%) of an orange solid that was washed with diethyl ether and dried in vacuo. Elemental Anal. Calcd for $C_{18}H_{30}Cl_2N_6O_2Pd$ (M = 539.80 g mol^{-1}): C, 40.05; H, 5.60; N, 15.57. Found: C, 40.54; H, 4.81; N, 15.09%. M.p. 193–195 °C. **IR** (ATR, cm^{-1}): ν = 3375 s (ν_{N-H}), 1665 m, 1635 s ($\nu_{C=O}$), 1564 s (ν_{C-N} + δ_{CNH}), 1519 w, 1464 w, 1439 m, 1414 m, 1386 w, 1356 m, 1344 w, 1318 w, 1283 m, 1263 m, 1248 m, 1224 w, 1176 w, 1160 w, 1130 w, 1106 w, 1083 s, 1057 w, 1008 w, 988 w, 961 w, 939 w, 896 w, 840 w, 783 w, 768 vs, 714 w, 677 w, 621 m, 575 m, 518 w, 455 w, 417 m. **^{1}H NMR** (400 MHz, $CDCl_3$): δ = 0.92 (6H, d, J = 6.58 Hz, CH(CH_3)$_2$), 3.63 (2H, t, J = 6.23 Hz, α-CH_2), 3.84 (1H, sept, J = 6.58 Hz, CH(CH$_3$)$_2$), 5.06 (2H, t, J = 6.23 Hz, β-CH_2), 6.19 (2H, s, br, NH), 6.35 (1H, t, J = 2.58 Hz, 4-CH), 7.55 (1H, dd, J = 2.58 Hz, J = 0.89 Hz, 3-CH), 7.80 (1H, dd, J = 2.58 Hz, J = 0.89 Hz, 5-CH) ppm. **^{13}C NMR** (100 MHz, $CDCl_3$): δ = 22.3 (s, CH(CH$_3$)$_2$), 37.3 (s, α-CH$_2$), 41.3 (s, β-CH$_2$), 49.9 (s, CH(CH$_3$)$_2$, 107.4 (s, 4-CH), 135.7 (s, 3-CH), 143.3 (s, 5-CH), 168.0 (s, C=O) ppm.

4.1.10. Synthesis of $PdCl_2(Me_2PPA^{iPr})_2$ (10)

Me_2PPA^{iPr} (**4**(79 mg, 0.38 mmol) and dichloro(1,5-cyclooctadiene)palladium(II) (73 mg, 0.25 mmol) were dissolved in 20 mL of chloroform and stirred under nitrogen for three days. Evaporation of the solvent yielded 141 mg (94%) of orange crystals suitable for X-ray diffraction analysis. Elemental Anal. Calcd. for $C_{22}H_{38}Cl_2N_6O_2Pd$ (M = 595.91 g mol^{-1}): C, 44.34; H, 6.43; N, 14.10%. Found: C, 44.09; H, 6.22; N, 13.66. M.p. 226 °C. **IR** (ATR, cm^{-1}): ν = 3294 vs, 3143 w, 3064 w (ν_{N-H}); 2972 s, 2931 w (ν_{C-H}), 1668 vs ($\nu_{C=O}$), 1543 s ($\nu_{C-N} + \delta_{CNH}$), 1459 s, 1436 w, 1411 s, 1387 m, 1367 m, 1334 w, 1297 m, 1262 s, 1234 m, 1182 s, 1164 s, 1138 w, 1129 w, 1096b, 1070 w, 1044 w, 1018 w, 960 w, 920 w, 890 w, 866 w, 798 vs, 741 m, 674 s, 659 s, 639 m, 630 m, 596 m, 585 m, 573, 452 m, 434 m. **^{1}H NMR** (400 MHz, $CDCl_3$): δ = 0.90 (6H, d, J = 6.57 Hz, CH(CH_3)$_2$), 2.33 (3H, s, 5-CH_3), 2.83 (3H, s, 3-CH_3), 3.72 (2H, t, J = 6.32 Hz, α-CH_2), 3.81 (1H sept, J = 6.57 Hz, CH(CH_3)$_2$), 4.92 (2H, t, J = 6.32 Hz, β-CH_2), 5.89 (1H, s, 4-CH), 6.49 (2H, s, br, NH) ppm. **^{13}C NMR** (100 MHz, $CDCl_3$): δ = 12.0 (s, 5-CH_3), 15.2 (s, 3-CH_3), 22.2 (s, CH(CH_3)$_2$), 37.3(s, α-CH_2), 41.5 (s, β-CH_2), 45.6 (s, CH(CH_3)$_2$), 107.5 (s, 4-CH), 145.3 (s, 5-C-CH_3), 150.1 (s, 3-C-CH_3) , 168.3 (s, C=O) ppm.

4.1.11. Synthesis of $PdCl_2(PPA^{MOP})_2$ (11)

A solution of PPA^{MOP} (**5**; (172 mg, 0.72 mmol) and dichloro(1,5-cyclooctadiene)palladium(II) (104 mg, 0.36 mmol) in 40 mL of acetone was refluxed for 1 h under a nitrogen atmosphere. Volatile components were removed in vacuum and the remaining solid was recrystallized from methylene chloride/hexanes to yield 128 mg (54%) of compound **11**. Crystals suitable for X-ray diffraction were obtained by vapor diffusion of hexanes into an ethanol solution. Elem. Anal. Calcd. for $C_{24}H_{38}Cl_2N_6O_4Pd$ (M = 651.93 g mol^{-1}): C, 44.22; H, 5.88; N, 12.89%. Found: C, 45.79; H, 6.28; N, 13.05. M.p. 139–141 °C. **IR** (ATR, cm^{-1}): ν = 3324 m (ν_{N-H}), 3144 m, 3120 m, 2975 m, 2962 m, 2927 m, 1715 vs ($\nu_{C=O}$, MOP), 1658 vs ($\nu_{C=O}$), 1518 m ($\nu_{C-N} + \delta_{CNH}$), 1456 m, 1418 m, 1384 m, 1353 m, 1336 m, 1209 m, 1140 m, 1075 m, 1042 m, 1017 w, 986 w, 951 w, 922 w, 903 w, 761 vs, 681 m, 647 m, 616 s, 576 s, 552 w, 541 w, 531 w, 516 w, 493 w, 480 w, 470 w, 459 w. **^{1}H NMR** (400 MHz, $CDCl_3$): δ = 1.20 (6H, s, C(CH_3)$_2$), 2.08 (3H, s, CH_3 (MOP)), 2.84 (2H, s, CH_2 (MOP)), 3.54 (2H, t, J = 6.24 Hz, α-CH_2), 5.05 (2H, t, J = 6.24 Hz, β-CH_2), 6.05 (1H, dd, J = 1.60 Hz, J = 1.25 Hz, 4-CH), 7.56 (1H, dd, J = 1.25 Hz, J = 0.50, 3-CH), 7.80 (1H, dd, J = 1.60 Hz, J = 0.50 Hz, 4-CH) ppm. **^{13}C NMR** (100 MHz, $CDCl_3$): δ = 26.8 (s, C(CH_3)$_2$), 31.6 (s, CH_3 (MOP)), 37.5 (s, α-CH_2), 49.6 (s, β-CH_2), 51.0 (s, CH_2 (MOP)), 52.3 (s, C(CH_3)$_2$), 107.3 (s, 5-CH), 135.5 (s, 3-CH), 143.1 (s, 5-CH), 168.6 (s, C=O), 207.1 (s, C=O (MOP)) ppm.

4.1.12. Synthesis of $PdCl_2(Me_2PPA^{MOP})_2$ (12)

A mixture of Me_2PPA^{MOP} (**6**; 235 mg, 0.89 mmol) and dichloro (1,5-cyclooctadiene)palladium(II) (117 mg, 0.41 mmol) in 15 mL of chloroform was refluxed for 1 hour producing an amber solution. The solvent was evaporated and 287 mg (86%) of compound **12** remained as a yellow solid. X-Ray quality crystals were obtained by vapor diffusion of pentanes into a chloroform solution. Elem. Anal. Calcd. for $C_{28}H_{46}Cl_2N_6O_4Pd$ (M = 708.04 g mol^{-1}): C, 47.50; H, 6.55; N, 11.87. Found: C, 47.13; H, 6.12; N, 11.74%. M.p. 199–201 °C. **IR** (ATR, cm^{-1}): ν = 3339 w (ν_{N-H}), 3001 w, 2975 w (ν_{C-H}), 1714 m ($\nu_{C=O}$, MOP), 1661 vs ($\nu_{C=O}$), 1556 w, 1533 m, 1470 w, 1461 w, 1436 w, 1403 w, 1361 s, 1303 w, 1261 w, 1234 w, 1183 w, 1158 w, 1067 w, 1045 w, 1006 w, 976 w, 956 w, 917 w, 900 w, 805 w, 796 w, 652 w, 624 w, 606 w, 580 w, 551 w, 542 w, 533 w, 528 w, 513 w, 509 w, 492 w, 484 w, l478 w, 474 w, 467 w. **H NMR** (400 MHz, $CDCl_3$): δ = 1.17 (6H, s, C(CH_3)$_2$), 2.07 (3H, s CH_3 (MOP)), 2.33 (3H, s, 5-CH_3), 2.83 (3H, s, 3-CH_3), 2.85 (2H, s, CH_2 (MOP)), 3.68 (2H, t, J = 6.2 Hz, α-CH_2), 4.90 (2H, t, J = 6.2 Hz, β-CH_2), 5.90 (1H, s, 4-CH), 6.52 (2H, s, br, NH) ppm. **^{13}C NMR** (100 MHz, $CDCl_3$): δ = 11.8 (s, 5-CH_3), 15.1 (s, 3-CH_3), 26.5 (s, C(CH_3)$_2$), 31.5 (s, CH_3 (MOP)), 37.7 (s, α-CH_2), 45.4 (s, β-CH_2), 51.0 (s, CH_2 (MOP)), 52.1 (s, C(CH_3)$_2$), 107.3 (s, 4-CH), 145,1 (s, 5-C-CH_3), 150.3 (s, 3-C-CH_3), 169.1 (s, C=O), 206.9 (s, C=O (MOP)) ppm.

Acknowledgments

The material is based on work supported by the National Science Foundation – United States under CHE-1062629 and 1461175. General financial support of this work by the Otto-von-Guericke-Universität Magdeburg is also gratefully acknowledged.

Appendix A

CCDC 1912534–1912540 (*cf.* Table 1) contains the supplementary crystallographic data for the compounds reported in this paper. These data can be obtained free of charge via http://www.ccdc.cam.ac.uk/conts/retrieving.html, or from the Cambridge Crystallographic Data Centre, 12 Union Road, Cambridge CB2 1EZ, UK; fax: (+44) 1223-336-033; or e-mail: deposit@ccdc.cam.ac.uk.

References

[1] S. Bhattacharya, A. Goswami, B. Gole, S. Ganguly, S. Bala, S. Sengupta, S. Khanra, R. Mondal, Construction of Bis-pyrazole Based Co(II) Metal-Organic Frameworks and Exploration of Their Chirality and Magnetic Properties, Cryst. Growth Des. 14 (2014) 2853.
[2] S. Bala, S. Bhattacharya, A. Goswami, A. Adhikary, S. Konar, R. Mondal, Designing Functional Metal-Organic Frameworks by Imparting a Hexanuclear Copper-Based Secondary Building Unit Specific Properties: Structural Correlation With Magnetic and Photocatalytic Activity, Cryst. Growth Des. 14 (2014) 6391.
[3] G.-N. Liu, M.-J. Zhang, W.-Q. Liu, H. Sun, X.-Y. Li, K. Li, C.-Z. Ren, Z.-W. Zhang, C. Li, Structures and multiple properties of two polar metal-organic frameworks based on achiral N,O-coordinated ligands: toward multifunctional materials, Dalton Trans. 44 (2015) 18882.
[4] S. Bhattacharya, S. Bala, R. Mondal, Design of chiral Co(II)-MOFs and their application in environmental remediation and waste water treatment, RSC Adv. 6 (2016) 25149.
[5] T. Jing, L. Chen, F. Jiang, Y. Yang, K. Zhou, M. Yu, Z. Cao, S. Li, M. Hong, Fabrication of a Robust Lanthanide Metal-Organic Framework as a Multifunctional Material for Fe(III) Detection, CO_2 Capture, and Utilization, Cryst. Growth Des. 18 (2018) 2956.
[6] A.-X. Tian, M.-L. Yang, N. Sun, Y.-B. Fu, J. Ying, A series of pH-dependent POM-based compounds as photocatalysts and electrochemical sensors, Polyhedron 155 (2018) 337.
[7] M. Roy, A. Adhikari, A.K. Mondal, R. Mondal, Multifunctional Properties of a 1D Helical Co(II) Coordination Polymer: Toward Single-Ion Magnetic Behavior and Efficient Dye Degradation, ACS Omega 3 (2018) 15315.
[8] F. Mani, Model systems containing pyrazole chelates and related groups: recent developments and perspectives, Coord. Chem. Rev. 120 (1992) 325.
[9] A.-S. Chauvin, Y.-M. Frapart, J. Vaissermann, B. Donnadieu, J.-P. Tuchagues, J.-C. Chottard, Y. Li, Inorg. Chem. 42 (2003) 1895.
[10] M. Sallmann, C. Limberg, Utilizing the Trispyrazolyl Borate Ligand for the Mimicking of O_2-Activating Mononuclear Nonheme Iron Enzymes, Acc. Chem. Res. 48 (2015) 2734.
[11] K.B. Girma, V. Lorenz, S. Blaurock, F.T. Edelmann, Coordination chemistry of acrylamide. 6 synthesis and coordination compounds of *N*-pyrazolylpropanamide – a versatile acrylamide-derived ligand, Z. Anorg. Allg. Chem. 634 (2008) 267.
[12] T. Wagner, C.G. Hrib, V. Lorenz, F.T. Edelmann, J.W. Gilje, Bromidobis[3-(1H-pyrazol-1-yl-κN^2)propionamide-κO]copper(II) bromide methanol monosolvate, Acta Cryst. E 68 (2012) m1253.
[13] T. Wagner, C.G. Hrib, V. Lorenz, F.T. Edelmann, D.S. Amenta, C.J. Burnside, J.W. Gilje, *N*-Pyrazolylpropanamide – a Versatile Ligand for the Construction of Supramolecular Hydrogen-Bonded Frameworks, Z. Anorg. Allg. Chem. 638 (2012) 2129.
[14] D.J. D'Amico, M.A. McDougal, D.S. Amenta, J.W. Gilje, S. Wang, C.G. Hrib, F.T. Edelmann, Synthesis and supramolecular structures of manganese complexes with *N*-pyrazolylpropanamide-derived ligands, Polyhedron 88 (2015) 19.
[15] P. Liebing, L. Wang, J.W. Gilje, L. Hilfert, F.T. Edelmann, Supramolecular first-row transition metal complexes of 3-(3,5-dimethylpyrazol-1-yl)propanamide: Three different coordination modes, Polyhedron 164 (2019) 228.
[16] T. Wagner, C.G. Hrib, V. Lorenz, F.T. Edelmann, J. Zhang, Q. Yi, *N*-Triazolylpropanamide – an Acrylamide-Derived Multifunctional Ligand for

the Construction of Supramolecular Hydrogen-Bonded Networks, Z. Anorg. Allg. Chem. 638 (2012) 2185.
[17] P. Liebing, L. Wang, J.W. Gilje, M. Kühling, F.T. Edelmann, A Polymorphic Gold (III) Complex Comprising a Multifunctional Triazolylpropanamide Ligand, Z. Anorg. Allg. Chem. 644 (2018) 270.
[18] S. Wang, P. Liebing, F. Oehler, J.W. Gilje, C.G. Hrib, F.T. Edelmann, Supramolecular Layer Structures of Mn(II), Co(II), and Cu(II) Complexes with the 3-(1*H*-Benzotriazol-1-yl)propaneamide Ligand: Metal Coordination vs Hydrogen Bonding, Cryst. Growth Des. 17 (2017) 3402.
[19] C.G. Hrib, F.T. Edelmann, C.W. Smith IV, K.C. McQueen, S.S. Cruz, D.S. Amenta, J. W. Gilje, $RuCl_2(PPh_3)_2$(*N*-ppa) – A Hydrogen-Bridged Ruthenium(II) Complex of *N*-Pyrazolylpropanamide, Z. Anorg. Allg. Chem. 639 (2013) 2561.
[20] T. Miyazawa, E.R. Blout, The Infrared spectra of Polypeptides in Various Conformations: Amide I and II Bands, J. Am. Chem. Soc. 83 (1961) 712.
[21] J.-F. Zhang, F. Huang, S.-J. Chen, 3-(3,5-Dimethyl-1H-pyrazol-1-yl)-propanamide, Acta Cryst. E65 (2009) o2442.
[22] C.J. Adams, M.F. Haddow, R.J.I. Hughes, M.A. Kurawa, A.G. Orpen, Coordination chemistry of platinum and palladium in the solid-state: Synthesis of imidazole and pyrazole complexes, Dalton Trans. 39 (2010) 3714.
[23] Stoe Stoe & Cie 2002, X-Area and X-Red, Stoe & Cie, Darmstadt, Germany.
[24] A. Altomare, M.C. Burla, M. Camalli, G.L. Cascarano, C. Giacovazzo, A. Guagliardi, A.G.G. Moliterni, G. Polidori, R. Spagna, SIR97: a new tool for crystal structure determination and refinement, J. Appl. Cryst. 32 (1999) 115.
[25] G.M. Sheldrick, SHELXT – Integrated space-group and crystal-structure determination, Acta Cryst. A71 (2015) 3.
[26] G.M. Sheldrick, Crystal structure refinement with SHELXL, Acta Cryst. C71 (2015) 3.